

# 論文 Seismic Behavior of Precast Shear Wall with Bar Splices Confined to Spiral Steel

Jose Caringal ADAJAR<sup>\*1</sup>, Teruaki YAMAGUCHI<sup>\*2</sup> and Hiroshi IMAI<sup>\*3</sup>

**ABSTRACT:** Two monolithic and five precast shear walls were subjected to cyclic anti-symmetrical bending moments and a constant axial load. The location of main bar connection and the type of concrete joint were the varied factors. By investigating the crack formation, load-displacement hysteretic relations, flexural and shear strengths, strain distribution on steel reinforcements, deformation components, and the slippage at the horizontal concrete joint, the seismic behavior of precast walls were compared to their monolithic counterparts.

**KEYWORDS:** precast shear wall, main bar connection, spiral steel, tubular steel sheath, lap splice, load-displacement relations, strain distribution, shear strength, slippage, deformation components

## 1. INTRODUCTION

This paper presents some informative data about the seismic performance of precast shear wall with a newly developed main bar connection. As shown in Fig. 1, this connection uses tubular spiral steel sheath to contain the main bar and the high strength grout filler. Four lap splice bars around the sheath are confined to small diameter (6 mm) spiral steel. After investigating some basic properties of the spirally confined bar splice subjected to direct pullout tests [1],[2], precast shear walls incorporating this type of splicing were tested. Conforming to the standard specifications in Japan, a splice length of 30 times the lapped bar diameter (30d) was used in this preliminary full scale member test.

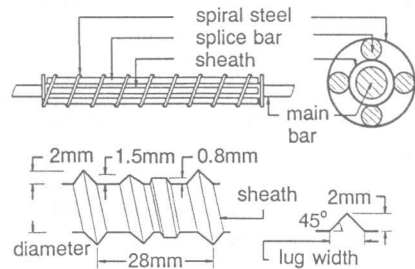


Fig. 1 Design of connection

## 2. EXPERIMENTAL INVESTIGATION

### 2.1 SPECIMENS AND MATERIAL PROPERTIES

The details of seven test specimens appear in Table 1. Each wall measures 200 cm high, 140 cm wide, and 15 cm thick. Two of the specimens designated as RCW1 and RCW3 are monolithically cast and the other five, which are named PCW2, PCW4, PCW5, PCW6 and PCW7, are prefabricated (designation: RC for monolithic and PC for precast). PCW2 is similar to RCW1 except that it has bar connections and horizontal concrete joint. The sketches of these two walls can be seen in Figs. 2(a) and 2(b). Having only 4-D25(SD345) main vertical reinforcements, these two specimens are designed

<sup>\*1</sup> Institute of Engineering Mechanics, University of Tsukuba, Graduate student, Member of JCI

<sup>\*2</sup> Technical Research Institute, Kabuki Construction Co, Member of JCI

<sup>\*3</sup> Institute of Engineering Mechanics, University of Tsukuba, DR, Member of JCI

for bending failure. The main bar connections in PCW2 are located near the bottom end and the horizontal concrete joint is *mortar seal* designed for internal walls.

RCW3 is a monolithic wall with seven D25(SD390) main vertical bars. Four precast walls, namely, PCW4, PCW5, PCW6, and PCW7 are similar to RCW3 except that their main bars are connected at mid-height of the walls. The sketches are drawn in Figs. 3(a) and 3(b). Also, in these four

precast walls, the type of horizontal concrete joint varies. As shown in Figs. 4(a) and 4(b), PCW4 uses *mortar seal* for internal wall while that of PCW5 is also *mortar seal* but for external wall. In PCW6, *laid mortar* method which is illustrated in Fig. 4(c) is employed and PCW7 is connected using *all-grout* method shown in Fig. 4(d).

The specified compressive strength for concrete was 300 kgf/cm<sup>2</sup> and 600 kgf/cm<sup>2</sup> for grout but the actual concrete compressive strength turned out to be higher especially in the monolithic walls. Tables 2(a), 2(b) and 2(c) show the actual compressive strengths of concrete, grout, and mortar, respectively. The actual strengths of the steel bars are higher than the specified ones and these are tabulated in Table 2(d).

## 2.2 CONSTRUCTION METHOD

Monolithic walls, RCW1 and RCW3, were cast horizontally at the testing laboratory. The rest were prefabricated in the precast concrete factory and were jointed in the laboratory. In the fabrication of precast walls, main bars were not included. Instead, tubular spiral steel sheaths were placed on their locations to provide openings for the main bars. The four lapped bars around a main bar connection, the confining spiral steel, and the horizontal and vertical web reinforcements were on their positions during casting of concrete. Trapezoidal groove was provided at the bottom of each wall to serve as

Table 1 Details of specimens

Specimen number	Designed failure	RC/PCa	Location of bar connection	Type of concrete connection	Axial stress (kgf/cm <sup>2</sup> )	Mesh reinf.	Main Bar
RCW1	flexural	RC	-	-	5.0	2-D10 @200mm	4-D25 (SD345)
PCW2	"	PCa	bottom	mortar seal (inner wall)	"	"	"
RCW3	shear	RC	-	-	"	"	7-D25 (SD390)
PCW4	"	PCa	middle	mortar seal (inner wall)	"	"	"
PCW5	"	"	"	mortar seal (outer wall)	"	"	"
PCW6	"	"	"	laid mortar	"	"	"
PCW7	"	"	"	all-grout	"	"	"

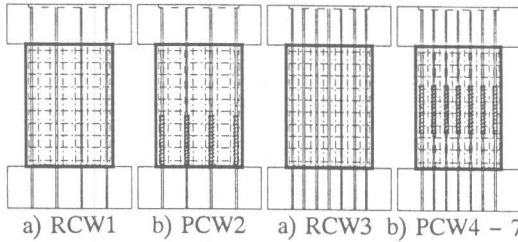


Fig. 2 Flexural failure type specimens

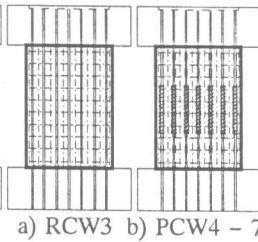


Fig. 3 Shear failure type specimens

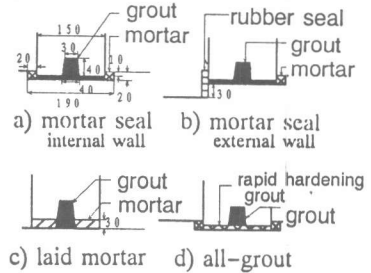


Fig. 4 Types of horizontal concrete joints

Table 2 Material test results

a) concrete	(kgf/cm <sup>2</sup> )			b) grout	(kgf/cm <sup>2</sup> )		
	28 days	Day of experiment	Compression		No. of days	7	28
RCW1	387	477	30	Compression	515	677	762
PCW2	318	389	34				
RCW3	387	472	32				
PCW4	274	330	31				
PCW5	284	339	29				
PCW6	257	328	25	c) mortar	(kgf/cm <sup>2</sup> )		
PCW7	281	328	29		No. of days	3	7
				Compression	248	365	510
d) steel				(tonf/cm <sup>2</sup> )			
Size/Specs.	Yield	Actual Yield	Max. Tensile	Remarks			
D25(SD390)	4.0	4.75	6.37	main bar			
D25(SD345)	3.5	3.81	5.82	main bar			
D13(SD345)	3.5	3.85	5.66	splice			
D10(SD295A)	3.0	3.64	5.00	mesh			
φ6		5.38	5.94	spiral			

duct in order for the grout to enter into all the sheaths. The lower reaction beam with protruding vertical main bars was cast separately. The wall specimen and the upper reaction beam were cast together but openings for vertical bars were provided using the tubular steel sheaths.

In jointing the precast elements, the wall specimen together with the upper reaction beam were raised in such a way that the protruding main bars on the lower reaction beam can be inserted. Once these lower bars were set, the upper bars were inserted from the top reaction beam down into the wall until they touched the ends of the lower bars. The bottom of the wall was sealed with either mortar or grout depending on the type of horizontal concrete joint. The high strength grout was injected to fill all the sheaths at the same time from the bottom of the wall to the top reaction beam.

### 2.3 LOADING METHOD

As illustrated in Fig. 5, each specimen was subjected to cyclic anti-symmetrical bending moments and a constant axial stress of  $5.0 \text{ kgf/cm}^2$ . The drift angle  $R$  caused by the lateral force was doubled after every two cycles as illustrated in Fig. 6.

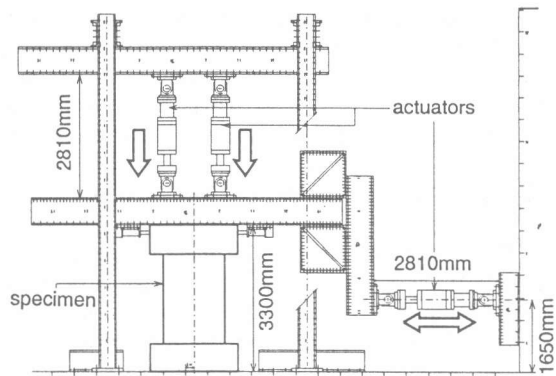


Fig. 5 Loading apparatus

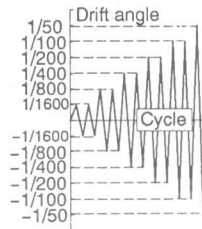


Fig. 6 Loading history

### 2.4 STRAIN GAUGES AND DISPLACEMENT TRANSDUCERS

The relative displacement between the top and bottom of each wall was measured at mid-height using two CDP gauges (accuracy:  $1000\mu\text{/mm}$ ) and two SDP gauges ( $100\mu\text{/mm}$ ). The slippage at each end of the specimen was monitored using three CDP gauges. Twelve pi gauges ( $1000\mu\text{e/mm}$ ) for flexural deformation measurement and thirteen CDP gauges ( $500\mu\text{/mm}$ ) for shear deformation were installed. Sixty three strain gauges were distributed on the steel reinforcements of every specimen except PCW2 which had 65 strain gauges.

## 3. TEST RESULTS AND DISCUSSION

### 3.1 CRACK FORMATION

In RCW1 and PCW2 which are designed for flexural failure, only flexural cracks occurred at the ends of the wall from a drift angle  $R$  of  $1/1600$  until  $1/800$ . Diagonal shear cracks started to appear before  $R$  reaches  $1/400$  and propagated until  $R = 1/50$ . In every cycle, the formation of cracks in the precast wall PCW2 was identical to that of the monolithic wall RCW1. At failure, RCW1 crushed at the lower end portion unlike PCW2 which broke at both lower end corners as can be seen in Fig. 7. This was due to the additional stiffness contributed by the lapped bars to the lower portion of the wall which helped minimized bending on that portion.

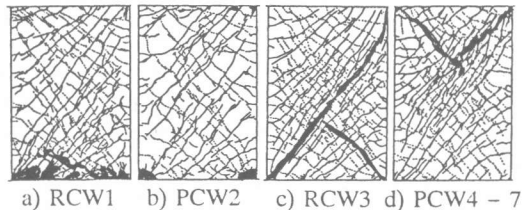


Fig. 7 Crack patterns

In the shear failure type specimens, within an angle of  $1/1600$  only flexural cracks were noticed.

The occurrence of diagonal cracks was early at  $R=1/800$ . At this stage, the central portion of the monolithic wall RCW3 remains uncracked while those of the precast elements were cracked. Within  $R = 1/400$  and  $1/200$ , the crack formations in both monolithic and precast specimens were similar. At failure, within  $R = 1/100$ , RCW3 collapsed at the corner to corner diagonal crack while the precast ones broke at the upper third portion above the lapped bars shown in Fig. 7.

### 3.2 LOAD-DISPLACEMENT RELATIONS

The hysteresis curves of all the specimens are plotted in Fig. 8. RCW1 reached the maximum load only once at  $R = 1/100$  and its strength decayed gradually on the succeeding driftage. Its precast counterpart PCW2 behaved in somewhat ductile manner for it was able to attain the maximum load level thrice at  $R = 1/200$ ,  $1/100$  and  $1/50$ . After reaching the highest load at  $R = 1/50$ , the wall collapsed and was not able to recover much strength in the opposite direction of the cycle. All shear failure specimens, RCW3 and PCW4-7, had similar hysteretic behavior as shown in Fig. 8. The maximum load was reached either at a drift angle of  $1/200$  or before reaching  $1/100$ . After reaching the highest load while drifting to angle  $1/100$ , the load of a specimen suddenly decreased to about 70 to 80 percent of the highest load when the angle  $1/100$  was attained.

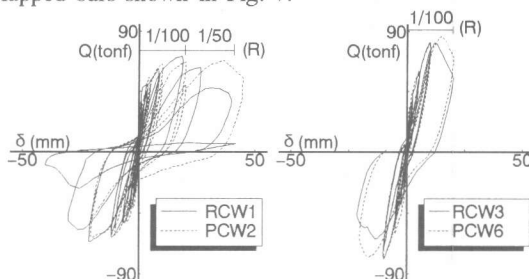


Fig. 8 Load - displacement hysteretic relations

### 3.3 FLEXURAL AND SHEAR STRENGTHS

Table 3 Experimental and calculated flexural and shear strengths

Specimen	Experimental lateral force, $Q_{max}$	Designed type of failure	Lateral force from theoretical bending moment		Lateral force from theoretical shear strength		
			Japanese	Park & Paulay	AIJ(A method)	ACI prov.	Park & Paulay
RCW1	71.6	flexure	54.3	61.4	97.7	72.7	68.3
PCW2	68.5	flexure	54.3	61.4	90.4	69.0	66.6
RCW3	82.1	shear	104.0	125.3	97.2	72.5	70.8
PCW4	82.6	shear	104.0	125.3	82.9	66.4	66.2
PCW5	84.3	shear	104.0	125.3	84.3	66.9	69.0
PCW6	86.6	shear	104.0	125.3	82.9	66.4	66.2
PCW7	86.3	shear	104.0	125.3	82.9	66.4	66.2

Table 3 shows the experimental and calculated strengths. For RCW1 and PCW2, the shear forces calculated from the theoretical bending moments [3],[4] are lesser than the experimental values. The maximum capacity of RCW1 is slightly higher than that of PCW2 because RCW1 has higher concrete compressive strength. RCW1 and PCW2 did not collapse after yielding of main bars. Their main bars were able to sustain more loads until the shear reinforcements yielded. The actual maximum lateral loads in PCW4 - 7 agree well with the values calculated using the equation [3] developed by AIJ based on the Arch and Truss theory, but that of RCW3 is much lower than the calculated ones. The difference is that RCW3 had  $F_c = 477 \text{ kgf/cm}^2$  while PCW4 - 7 had about  $330 \text{ kgf/cm}^2$ . Besides, the component materials, such as, sheath, grout, splice bars and spiral steel, change the configuration of the inner section of the wall. Although PCW4 - 7 has lower concrete compressive strength, they were able to resist higher shear forces than RCW3. This fact suggests a further verification on the applicability of AIJ equation in calculating the shear strength of shear walls with high strength concrete and with different sectional configuration. The results obtained using other equations [4],[5] are far from the experimental values.

### 3.4 STRAIN DISTRIBUTIONS ON STEEL REINFORCEMENTS

In discussing the strain distributions, the strains at the first peak of each positive cycle were used. The outermost main bars of RCW1 and PCW2 became highly stressed at the end portions only when

the external lateral force, as shown in Fig. 9, was maximum. That was when the deflection angle was 1/100. In the previous cycles, the middle portion of the bar in PCW2 which was about 50% of the height remained almost unstressed while there was an increasing strain in the lower middle portion of RCW1. The strain was still below the yield point. Strains on the lapped bars plotted in Fig. 9(b) show that there was an effective transfer of force between jointed bars. In the shear-failure type specimens, the strain distributions on the outermost bars shown in Fig. 10 were identical both for monolithic wall RCW3 and its precast counterparts PCW4 to PCW7. Only the end portion yielded at  $R = 1/100$ . Lapped bars transferred effectively the load on the joint. This can be concluded from the strain values of lapped splices shown in Fig. 10(b) and the strains on the main bars.

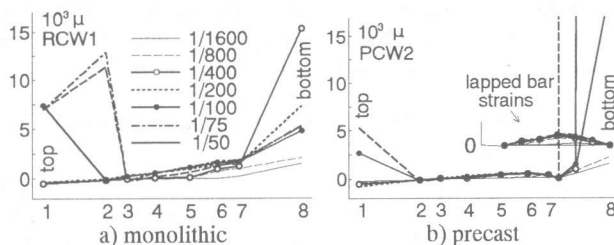


Fig. 9 Outermost main bar distribution (bending-failure type)

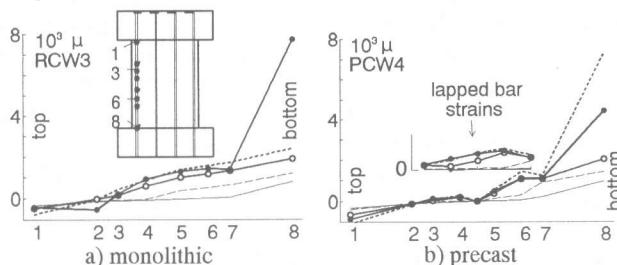


Fig. 10 Outermost main bar distribution (shear-failure type)

The section at the top end of RCW1 remained plane until  $R = 1/400$  while that of PCW2 remained plane until  $R = 1/200$  as can be seen in Fig. 11(a). At high load levels, the bars across the end sections were all in tension. In RCW3 and PCW4-7, the upper section remained plane until  $R = 1/200$  as shown also in Fig. 11(b). These were verified using the strains of main bars on those sections.

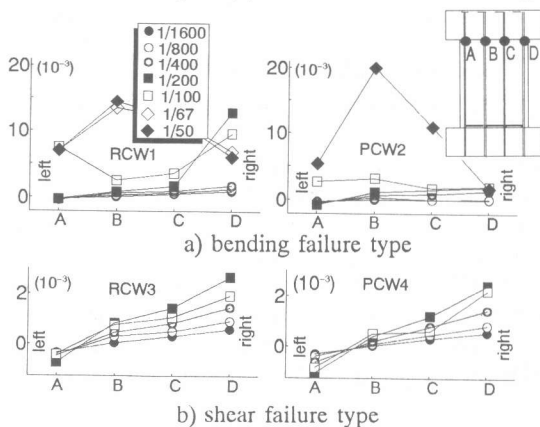


Fig. 11 Strain at the top end section

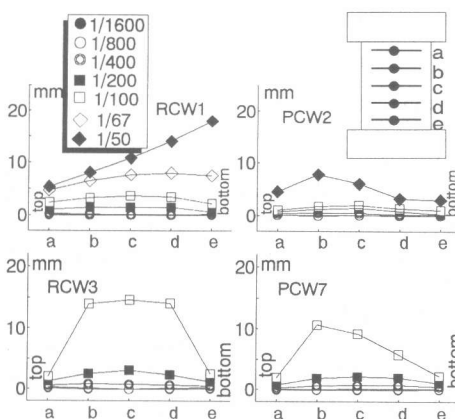


Fig. 12 Lateral expansion of specimens

As shown in Fig. 12, the lateral expansion of RCW1 reached almost 20 mm at the lower end while that of PCW2 was only 8.0 mm. Fig. 12 also illustrates that the lateral expansion of RCW3, which was 15 mm at mid-height, was evenly distributed along the middle half portion of the height and that of precast walls was only 8.0 to 12.0 mm on the upper quarter portion. Compared to the monolithic wall RCW1, PCW2 performed better in preventing lateral expansion because of the additional rigidity provided by the confined grout and the lapped bars at the lower portion of the wall. The expansion at the middle half of RCW3 was bigger than that in PCW4 - 7 because the grout and the lapped bars acted as stiffeners. Except PCW5, the lateral expansion of the top and bottom ends were almost zero.

The anchorage of main bars to the reaction beams prevented the ends from widening. In all the tested precast specimens, the highest strain on the spiral steel occurred in PCW2 where the main bars were highly stressed. This maximum strain was still below half of the yield strain of spiral steel.

### 3.5 SLIPPAGE AT THE CONSTRUCTION JOINT

The average slippage at the bottom of RCW1, which includes the shear deformation of the portion 50 mm below the point of measurement, was 6.5 mm while that of PCW2 was 13.8mm. The slippage in RCW1 was lesser because the vertical mesh reinforcements were embedded by about 3.0 cm in the reaction beam. Additional anchorage caused by these mesh reinforcements minimized the slip. Slippage in RCW1 and PCW2 were considerably large because the dependable shear stress resistance of the horizontal joint was almost half the required shear strength at that level [4]. RCW3 and its precast counterparts had a slippage of 0.5 to 1.0 mm except PCW6 which incurred 4.0mm. There was a greater slip in PCW6 because the type of horizontal concrete joint used which was named *laid mortar* was not so effective in transmitting shear stress across the horizontal joint. The shear resistance provided by the seven main bars across the horizontal joint was slightly greater than the required shear strength [4]. That was why the slip in the shear-failure type specimens were relatively small.

### 3.6 DEFORMATION COMPONENTS

The total deformation consists of the flexural displacement, shear deformation and slippage. Figure 13 shows the deformation components of the specimens. RCW1 and PCW2 are different during the last stage in that flexural and shear deformations governed in RCW1 while in PCW2, the slippage and the shear deformation are large. For the shear-failure type specimens, the percentage deformations are similar.

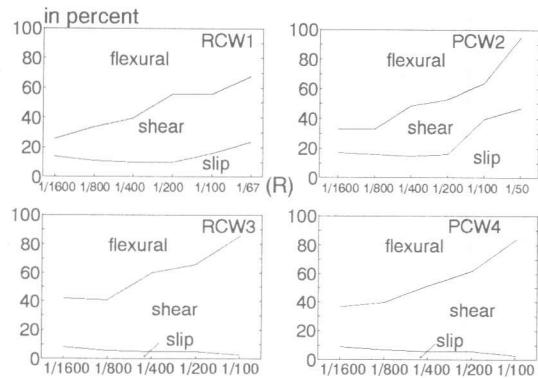


Fig. 13 Components of total deformation

### 4. CONCLUSIONS

In general, the seismic performance of precast walls with spirally confined bar connections are better than their monolithic counterparts. The lapped bars and the sheaths confining the grout become stiffeners which contribute rigidity to the precast walls. The type of horizontal concrete joint and the shear capacity of main bars across the horizontal joint govern the slippage. *Laid mortar* method is not so effective in minimizing slip. Four D25(SD345) provide only half the required shear strength across the horizontal joint. The bending-failure type specimens did not collapse after yielding of main bars, but only after attaining the ultimate shear resistance when the shear reinforcements yielded. The ratio of the actual to the experimental (*Method A* of AIJ) shear capacity of the shear-failure type precast walls is approximately 1.0.

### REFERENCES

1. Adajar, J.C., Yamaguchi, T. and Imai, H., "An Experimental Study on the Tensile Capacity of Vertical Bar Joints in a Precast Shear Wall", Transactions of JCI, Vol. 15, 1993, pp. 557-564.
2. Adajar, J.C., Yamaguchi, T. and Imai, H., "Tensile Capacity of Main Bar Splice at a Reduced Precast Shear Wall Thickness", Transactions of JCI, 1994.
3. AIJ, "Structural Design Guidelines for RC Buildings (1994)", pp. 77-104.
4. Park, R. and Paulay, T., "Reinforced Concrete Structures", John Wiley & Sons, 1975, pp. 616-627.
5. ACI Committee 318, "Manual of Concrete Practice, Part 3", ACI, 1993, pp. 300-319.